Interaction and Multiscale Mechanics, Vol. 5, No. 3 (2012) 187-210 187
DOI: http://dx.doi.org/10.12989/imm.2012.5.3.187

Behavior of cable-stayed bridges built over faults

I.G. Raftoyiannis*, G.T. Michaltsos and T.G. Konstantakopoulos

Department of Civil Engineering, National Technical University of Athens, Greece

(Received June 10, 2012, Revised July 7, 2012, Accepted August 2, 2012)

Abstract. Cable-stayed bridges are commonly used in modern bridge engineering for covering long spans. In some special cases, the designer is obliged to build such a bridge over an existing fault. Activation of this fault is possible to bring about a relative displacement or separation movement between two neighboring pylons of the bridge built on opposite sides of the fault. In this work, the effect of such a fault-induced pylon displacement on bridge's deformations and on cables' strength is thoroughly studied for several types of cable-stayed bridges and useful conclusions are drawn aiming the design. The influence of a possible earthquake and traffic loads crossing the bridge when the pylons are moving away from each other is not examined.

Keywords: cable-stayed bridges; pylon displacement; fault; fault-induced pylon movement.

1. Introduction

Cable-stayed bridges have been developed since the beginning of the 18^{th} century as described by Leonard (1972), but they have been of great interest only in the last 50 years, particularly due to their special shape and also because they constitute an alternative solution to suspension bridges for covering long spans (Troitsky 1988). The main reasons for their late application were difficulties in their static and dynamic analysis, various non-linearities, absence of computational capabilities, as well as lack of high strength materials and construction techniques. Modern aspects on theory and design of cable-stayed bridges can be found in the book by Xanthakos (1994). In the international bibliography, one can find numerous studies concerning the static behavior of cable-stayed bridges, such as the studies by Fleming (1979), Kollbruner *et al*. (1980), Bruno and Grimaldi (1985), Gimsing (1997), Khalil (1999), Virgoreux (1999), Michaltsos *et al*. (2003) and Freire *et al*. (2006). Among other studies concerning the dynamic analysis of cable-stayed bridges are the ones by Fleming and Egeseli (1980), Nazmy and Abdel-Ghaffar (1990), Abdel-Ghaffar and Khalifa (1991), Chatterjee *et al*. (1994), Bruno and Golotti (1994), Achkire and Preumont (1996), Michaltsos (2001), Konstantakopoulos *et al*. (2002), Wang *et al*. (2010) and Mozos and Aparicio (2010). Stability aspects of cable-stayed bridges are also studied by Ermopoulos *et al*. (1992), Bosdogianni and Olivari (1997), Michaltsos (2005) and Michaltsos *et al*. (2008). In all the above studies, pylon foundation and soil type are two essential parameters of concern in the design, which are usually taken to be of normal conditions.

* Corresponding author, Assistant Professor, E-mail: rafto@central.ntua.gr

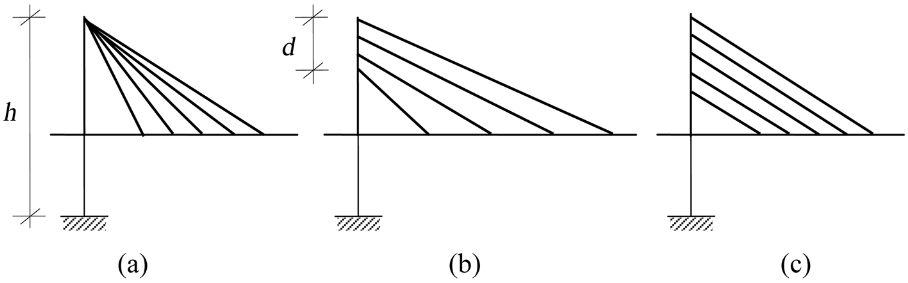

Fig. 1 Different systems of cables: (a) Fan, (b) Harp and (c) Parallel

In some special cases though, the designer is often obliged to build a bridge over an existing fault. Thus, there is a permanent danger of fault activation. This activation, besides the produced earthquake, is possible to bring about a relative displacement between two neighboring pylons of the bridge that are built on either side of the fault, Tapponnier *et al*. (2001) and Micarelli *et al*. (2006). This is not a theoretical case only. One typical example is that the new cable-stayed bridge "Charilaos Tricoupis" in Rion-Greece is built over such a fault and therefore, it is designed to be able to suffer significant displacements of its supports.

In the present work, the effect of such separation movements of pylons on a cable-stayed bridge and on its suspension system of cables is thoroughly studied using the method developed for the fan system by Michaltsos *et al*. (2003) and Michaltsos (2005), which is extended for the harp system as well. By this method, one can determine the relation between the forces of the cables and the deck's deformation and convert the problem to the solution of a continuous beam (i.e., the bridge deck) without cables. It should be stated at this stage that the influence of a possible earthquake occurring simultaneously with the above displacement of pylons is not examined. The influence of possible traffic loads crossing the bridge when the pylons are moving away from each other is not considered either.

As it is known, cable-stayed bridges are categorized from the static point of view into three basic types: the fan system (Fig. 1a), the harp system (Fig. 1b) and the parallel (Fig. 1c) system of cables, where the last one is a special case of the harp system. Regarding the second one, it is a common practice to place the cable anchors on the pylons (see Fig. 1b) within a short length d that is usually equal to $h/7$, thus achieving the greatest efficiency of the cables. As a consequence, a harp system of cables resembles rather to the fan system with total height equal to $(h\text{-}d/2)$ or $(h\text{-}d/3)$.

2. Statement of the problem

Let us consider the bridge of Fig. 2 built over a fault existing between pylons "a" and "b". The bridge is stayed by ρ cables at the left side of pylon "a" and the right side of pylon "b", and by κ cables at the right of pylon "a" and the left of pylon "b". Usually, in the harp system it is $\rho = \kappa$.

When the fault is activated, a relative horizontal displacement $e_1 + e_2$ occurs between the pylons. A relative vertical displacement also occurs, which is not considered herein but will included in a future research work. For the i-th cable in Fig. 2, one can write

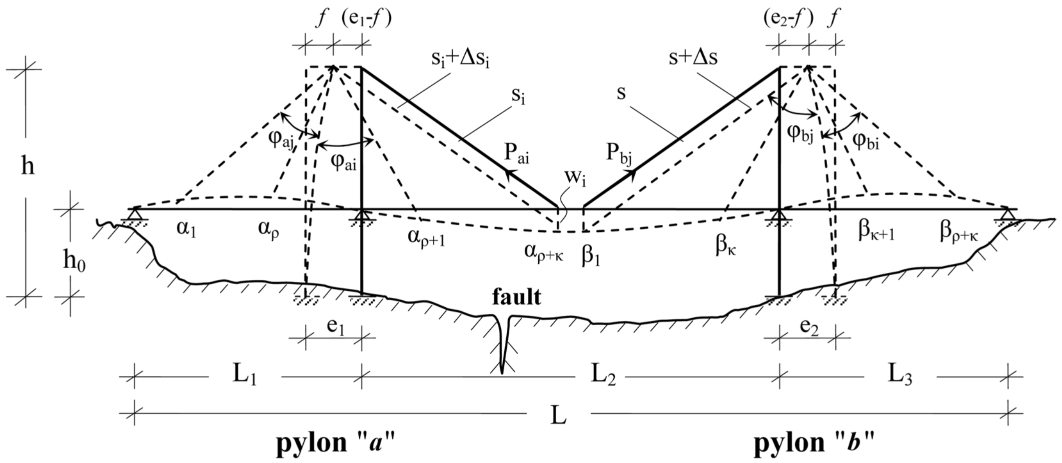

Fig. 2 Relative displacement of two neighboring pylons due to fault activation

$$\begin{aligned} s_i + \Delta s_i &= w_i \cos\varphi_i + s_i + (e_i - f)\sin\varphi_i \text{ or} \\ \Delta s_i + (f - e_i)\sin\varphi_i &= w_i \cos\varphi_i \end{aligned} \tag{1a}$$

Based on the relation $\Delta s_i = s_i P_i / E_c A_i$, the above Eq. (1a) becomes

$$\frac{s_i P_i}{E_c A_i} + (f - e_i)\sin\varphi_i = w_i \cos\varphi_i \tag{1b}$$

where E_c is the modulus of elasticity of the cables and A_i is the cross-sectional area of the i-th cable.

3. The fan system

3.1 Pylon's stressing

The deformation $f(z)$ at the point $A(z)$ of the pylon in Fig. 3 is: $E_p I_p(z) f'' = -P_x(z-h)$ or

$$\left.\begin{aligned} f'(z) &= -\int \frac{P_x(z-h)}{E_p I_p} dz + c_1 \\ f(z) &= -\int dz \int \frac{P_x(z-h)}{E_p I_p} dz + c_1 z + c_2 \end{aligned}\right\} \tag{2a}$$

The boundary conditions are: $f(0) = f'(0) = 0$. From Eq. (2a), one obtains

$$\left.\begin{aligned} & f = f_o(z) \cdot P_x \\ \text{where: } & f_o(z) = -\int dz \int \frac{P_x(z-h)}{E_p I_p} dz + \left[\int \frac{P_x(z-h)}{E_p I_p} dz\right]_{z=0} + \left[\int dz \int \frac{P_x(z-h)}{E_p I_p} dz\right]_{z=0} \end{aligned}\right\} \tag{2b}$$

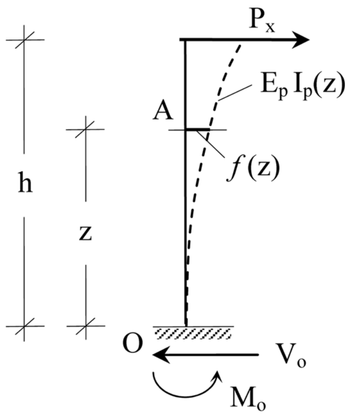

Fig. 3 Deformed configuration of the pylon

For $I_p(z) = I_p =$ constant, it will be $f(z) = -\frac{z^2(z-3h)}{6E_pI_p}$, which for $z = h$ gives

$$f_o = \frac{h^3}{3E_pI_p} \tag{2c}$$

3.2 Relation between P and w

3.2.1 Coarse arrangement of cables

The total deformation at the top of the pylon due to the horizontally acting forces is

$$f(h) = f_o(h)\Big[\sum_i P_i \sin\varphi_{ai} - \sum_j P_j \sin\varphi_{aj}\Big] \tag{3a}$$

Applying Eq. (1b) for both sides of the pylon, one obtains

$$\left.\begin{aligned}
&\text{left side } \frac{f_o}{b_j}\sin\varphi_{aj}\left(\sum_{j=1}^{\rho} P_j \sin\varphi_{aj} - \sum_{i=1}^{\kappa} P_i \sin\varphi_{ai}\right) + P_j - \frac{e_j \sin\varphi_{aj}}{b_j} = \frac{\cos\varphi_{aj}}{b_j} w_j \\
&\text{rigth side } \frac{f_o}{b_i}\sin\varphi_{ai}\left(\sum_{i=1}^{\kappa} P_i \sin\varphi_{ai} - \sum_{j=1}^{\rho} P_j \sin\varphi_{aj}\right) + P_i - \frac{e_i \sin\varphi_{ai}}{b_i} = \frac{\cos\varphi_{ai}}{b_i} w_i \\
&\text{where: } b_j = \frac{s_j}{E_cA_j} \quad and \quad b_i = \frac{s_i}{E_cA_i}
\end{aligned}\right\} \tag{3b}$$

Multiplying the first of Eq. (3b) by $\sin\varphi_{aj}$ and adding the ρ equations, and then multiplying the second of Eqs. (3.b) by $\sin\varphi_{ai}$ and adding the κ equations, one obtains the following relations

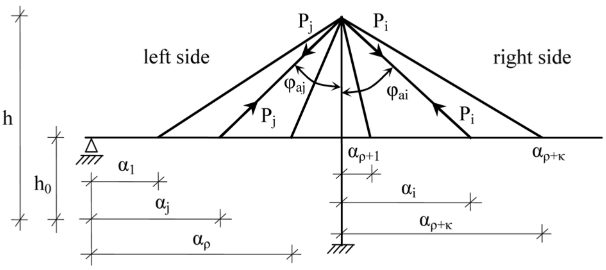

Fig. 4 Forces acting on the pylon due to the cables

left side

$$\left.\begin{array}{l} f_o\sum_{j=1}^{\rho}\frac{\sin^2\varphi_{aj}}{b_j}\left(\sum_{j=1}^{\rho}P_j\sin\varphi_{aj}-\sum_{i=1}^{\kappa}P_i\sin\varphi_{ai}\right)+\sum_{j=1}^{\rho}P_j\sin\varphi_{aj}-e_j\sum_{j=1}^{\rho}\frac{\sin^2\varphi_{aj}}{b_j}=\sum_{j=1}^{\rho}\frac{\sin2\varphi_{aj}}{2b_j}w_j \\ \text{right side} \\ f_o\sum_{i=1}^{\kappa}\frac{\sin^2\varphi_{ai}}{b_i}\left(\sum_{i=1}^{\kappa}P_i\sin\varphi_{ai}-\sum_{j=1}^{\rho}P_j\sin\varphi_{aj}\right)+\sum_{i=1}^{\kappa}P_i\sin\varphi_{ai}-e_i\sum_{i=1}^{\kappa}\frac{\sin^2\varphi_{ai}}{b_i}=\sum_{i=1}^{\kappa}\frac{\sin2\varphi_{ai}}{2b_i}w_i \end{array}\right\} \tag{3c}$$

Subtracting the above two equations from each other, one finally obtains

$$\left.\begin{array}{l} \Phi_a=\dfrac{1}{f_o(A_{aj}+A_{ai}+1)}\left\{\sum_{j=1}^{\rho}\frac{\sin2\varphi_{aj}}{2b_j}w_j-\sum_{i=1}^{\kappa}\frac{\sin2\varphi_{ai}}{2b_i}w_i\right\}+(e_jA_{aj}-e_iA_{ai}) \\ \text{where:}\quad \Phi_a=\sum_{j=1}^{\rho}P_j\sin\varphi_{aj}-\sum_{i=1}^{\kappa}P_i\sin\varphi_{ai},\quad A_{aj}=\sum_{j=1}^{\rho}\frac{\sin^2\varphi_{aj}}{b_j},\quad A_{ai}=\sum_{i=1}^{\kappa}\frac{\sin^2\varphi_{ai}}{b_i} \end{array}\right\} \tag{3d}$$

From Eq. (3b), one can easily obtain the cables' stresses as follows

$$\left.\begin{array}{l} P_j=\dfrac{\cos\varphi_{aj}}{b_j}w_j-f_o\dfrac{\sin\varphi_{aj}}{b_j}\Phi_a+e_j\dfrac{\sin\varphi_{aj}}{b_j} \\ P_i=\dfrac{\cos\varphi_{ai}}{b_i}w_i+f_o\dfrac{\sin\varphi_{ai}}{b_i}\Phi_a+e_i\dfrac{\sin\varphi_{ai}}{b_i} \end{array}\right\} \tag{3e}$$

3.2.2 Dense arrangement of cables

Let us consider next a dense arrangement of cables, as shown in Fig. 5, in which the distances δ_j and δ_i between two adjacent cables satisfy the following conditions

$$\delta_j \ll \alpha_\rho-\alpha_1 \quad \text{and} \quad \delta_i \ll \alpha_{\rho+\kappa}-\alpha_{\rho+1} \tag{4a}$$

Thus, we may consider a distributed load $q_z(x)$ applied from position α_1 to position α_ρ and from position $\alpha_{\rho+1}$ to position $\alpha_{\rho+\kappa}$, which at position "i" will be

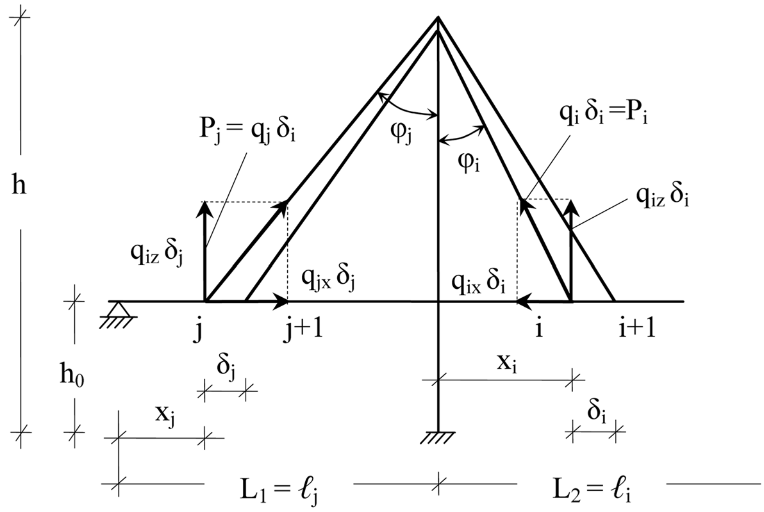

Fig. 5 Pylon force equilibrium due to a dense arrangement of cables

$$q_i(x) = \frac{1}{\delta_i} \cdot P_i \tag{4b}$$

Following the notations of Fig. 5, one has

$$\left.\begin{aligned} s_i &= \frac{h-h_o}{\cos\varphi_i}, \quad \sin\varphi_i = \frac{x_i}{\sqrt{(h-h_o)^2 + x_i^2}}, \quad \cos\varphi_i = \frac{h-h_o}{\sqrt{(h-h_o)^2 + x_i^2}} \\ s_j &= \frac{h-h_o}{\cos\varphi_j}, \quad \sin\varphi_j = \frac{\ell_j - x_j}{\sqrt{(h-h_o)^2 + (\ell_j - x_j)^2}}, \quad \cos\varphi_j = \frac{h-h_o}{\sqrt{(h-h_o)^2 + (\ell_j - x_j)^2}} \end{aligned}\right\} \tag{4c}$$

and through a similar process like the one of §3.2.1, one obtains for pylon "*a*"

$$\left.\begin{aligned} q_{aj}(x) &= \frac{\cos\varphi_{aj}}{b_{aj}} w_j - f_o \frac{\sin\varphi_{aj}}{b_{aj}} \Phi_a + e_j \frac{\sin\varphi_{aj}}{b_{aj}} \\ q_{ai}(x) &= \frac{\cos\varphi_{ai}}{b_{ai}} w_i + f_o \frac{\sin\varphi_{ai}}{b_{ai}} \Phi_a + e_i \frac{\sin\varphi_{ai}}{b_{ai}} \\ \text{where: } \Phi_a &= \frac{1}{f_o(I_{aj} + I_{ai} + 1)} \left[\int_{\alpha 1}^{\alpha\rho} \frac{\sin 2\varphi_{aj}}{2b_{aj}} w_j dx_1 - \int_{\alpha(\rho+1)}^{\alpha(\rho+\kappa)} \frac{\sin 2\varphi_{ai}}{2b_{ai}} w_i dx_2 + (e_i I_{ai} + e_j I_{aj}) \right] \\ I_{aj} &= \int_{\alpha 1}^{\alpha\rho} \frac{\sin^2\varphi_{aj}}{b_{aj}} dx_1, \quad I_{ai} = \int_{\alpha(\rho+1)}^{\alpha(\rho+\kappa)} \frac{\sin^2\varphi_{aj}}{b_{ai}} dx_2 \end{aligned}\right\} \tag{4d}$$

Similarly, for pylon "*b*" one obtains

$$\left.\begin{aligned}
q_{bj}(x) &= \frac{\cos\varphi_{bj}}{b_{bj}}w_j - f_o\frac{\sin\varphi_{bj}}{b_{bj}}\Phi_b + e_j\frac{\sin\varphi_{bj}}{b_{bj}} \\
q_{bi}(x) &= \frac{\cos\varphi_{bi}}{b_{bi}}w_i + f_o\frac{\sin\varphi_{bi}}{b_{bi}}\Phi_b + e_i\frac{\sin\varphi_{bi}}{b_{bi}} \\
\text{where: } \Phi_b &= \frac{1}{f_o(I_{bj}+I_{bi}+1)}\left[\int_{b1}^{b\kappa}\frac{\sin 2\varphi_{bj}}{2b_{bj}}w_j dx_2 - \int_{b(\kappa+1)}^{b(\kappa+\rho)}\frac{\sin 2\varphi_{bi}}{2b_{bi}}w_i dx_3 + (e_i I_{bi} + e_j I_{bj})\right] \\
I_{bj} &= \int_{b1}^{b\kappa}\frac{\sin^2\varphi_{bj}}{b_{bj}}dx_2, \quad I_{bi} = \int_{b(\kappa+1)}^{b(\kappa+\rho)}\frac{\sin^2\varphi_{bi}}{b_{bi}}dx_3
\end{aligned}\right\} \quad (4e)$$

4. The harp system

The harp system of cables is the most commonly used cable arrangement in bridge engineering (see Fig. 6). It is obvious that the change of the cables' direction should follow a law that is characteristic for the bridge.

The most commonly used law is the one shown in Fig. 6 according to which, the cables are anchored at one end at equal distances γ on the pylon, and at the other end at distances δ_ℓ on the left side of the deck or at distances δ_r on the right side of the deck. Easily, we can determine the following relations

$$\left.\begin{aligned}
\tan\varphi_{\rho\ell} &= \frac{\ell_\ell - x_{\rho\ell}}{h_\rho - h_o}, \quad \tan\varphi_{\rho r} = \frac{x_{\rho r}}{h_\rho - h_o} \\
s_{\rho\ell} &= \frac{\ell_\ell - x_{\rho\ell}}{\sin\varphi_{\rho\ell}}, \quad s_{\rho r} = \frac{x_r}{\sin\varphi_{\rho r}}
\end{aligned}\right\} \quad (5)$$

4.1 Pylon's stressing

The deformed state of a pylon subjected to horizontal forces due to the actions of cables is shown

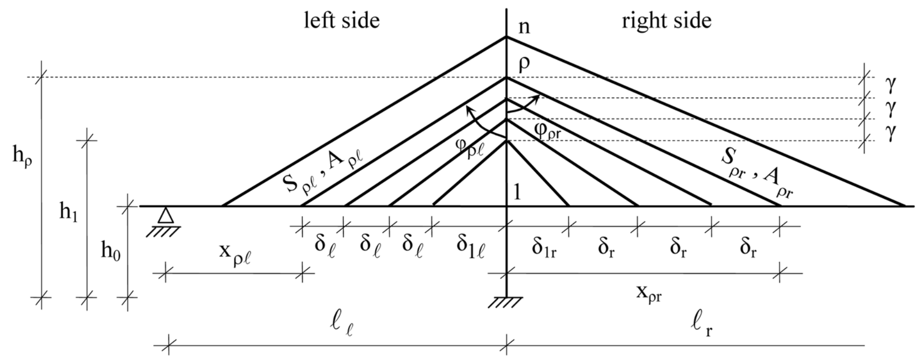

Fig. 6 Cable arrangement in a harp system

in Fig. 7. The produced reactions are

$$\left.V_o = \sum_1^n P_{x\rho}, \quad M_o = \sum_1^n h_\rho P_{x\rho}\right\} \tag{6a}$$

The displacements at each section of the pylon are given by the following relations

$$\left.\begin{aligned} EI_p f''_{\rho-1} &= M_o - zV_o + \sum_1^{\rho-2}(z-h_i)P_{xi} \quad \text{for} \ \ z \geq h_{\rho-2} \\ EI_p f''_\rho &= M_o - zV_o + \sum_1^{\rho-1}(z-h_i)P_{xi} \quad \text{for} \ \ z \geq h_{\rho-1} \end{aligned}\right\} \tag{6b}$$

The following conditions must be satisfied

$$\left. f'_{\rho-1}(h_{\rho-1}) = f'_\rho(h_{\rho-1}), \quad f_{\rho-1}(h_{\rho-1}) = f_\rho(h_{\rho-1})\right\} \tag{6c}$$

Integrating Eqs. (6b), one obtains

$$\left.\begin{aligned} EI_p f'_{\rho-1} &= zM_o - \frac{z^2}{2}V_o + \frac{z^2}{2}\sum_1^{\rho-2}P_{xi} - z\sum_1^{\rho-2}h_iP_{xi} + c_{\rho-1} \\ EI_p f'_\rho &= zM_o - \frac{z^2}{2}V_o + \frac{z^2}{2}\sum_1^{\rho-1}P_{xi} - z\sum_1^{\rho-1}h_iP_{xi} + c_\rho \end{aligned}\right\} \tag{6d}$$

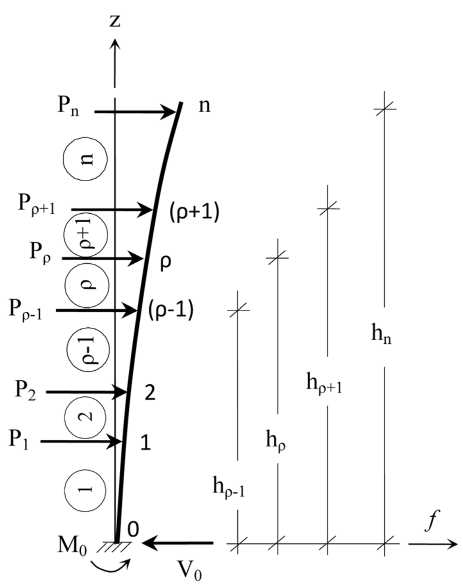

Fig. 7 Pylon stressing due to cables

The first condition of Eq. (6c) gives: $c_\rho = c_{\rho-1} + \frac{h_{\rho-1}^2}{2}P_{x(\rho-1)}$. Following a similar process, one finally obtains: $c_\rho = c_o + \frac{1}{2}\sum_1^{\rho-1} h_i^2 P_{xi}$. Since it is $f_1'(0) = 0$, one gets $c_o = 0$, and thus

$$c_\rho = \frac{1}{2}\sum_{i=1}^{\rho-1} h_i^2 P_{xi} \tag{6e}$$

After integration, Eq. (6d) become

$$\left.\begin{aligned} EI_p f_{\rho-1} &= \frac{z^2}{2}M_o - \frac{z^3}{6}V_o + \frac{z^3}{6}\sum_1^{\rho-2} P_{xi} - \frac{z^2}{2}\sum_1^{\rho-2} h_i P_{xi} + zc_{\rho-1} + k_{\rho-1} \\ EI_p f_\rho &= \frac{z^2}{2}M - \frac{z^3}{6}V_o + \frac{z^3}{6}\sum_1^{\rho-1} P_{xi} - \frac{z^2}{2}\sum_1^{\rho-1} h_i P_{xi} + zc_\rho + k_\rho \end{aligned}\right\}$$

Introducing the above into the second condition of Eq. (6c) and following a similar process, one finds

$$k_\rho = -\frac{1}{6}\sum_{i=1}^{\rho-1} h_i^3 P_{xi} \tag{6f}$$

Thus, one arrives at the following expression for the deformations of the pylon

$$\left. EI_p f_\rho(z) = -\frac{z^3}{6}\sum_{i=\rho}^{n} P_{xi} + \frac{z^2}{2}\sum_{i=\rho}^{n} h_i P_{xi} + \frac{z}{2}\sum_{i=1}^{\rho-1} h_i^2 P_{xi} - \frac{1}{6}\sum_{i=1}^{\rho-1} h_i^3 P_{xi} \quad \text{for} \quad z \geq h_{\rho-1} \right\} \tag{6g}$$

4.2 Relation between P and w

4.2.1 Coarse arrangement of cables

Setting: $$\left. a = \frac{1}{EI_p}, \quad b_{\rho\ell} = \frac{s_{\rho\ell}}{E_c A_{\rho\ell}}, \quad b_{\rho r} = \frac{s_{\rho r}}{E_c A_{\rho r}} \right\} \tag{7}$$

applying Eq. (1b), and employing Eq. (6g), one obtains the following relations

left side

$$a \sin^2\varphi_{\rho\ell}\left(\frac{h_\rho^3}{6b_{\rho\ell}}A_0 - \frac{h_\rho^2}{2b_{\rho\ell}}A_1 - \frac{h_\rho}{2b_{\rho\ell}}A_2 + \frac{1}{6b_{\rho\ell}}A_3\right) + \frac{e_i \sin^2\varphi_{\rho\ell}}{b_{\rho\ell}} + P_{x\rho\ell} = \frac{w_{\rho\ell}}{2b_{\rho\ell}}\sin 2\varphi_{\rho\ell}$$

right side (8a)

$$a \sin^2\varphi_{\rho r}\left(-\frac{h_\rho^3}{6b_{\rho r}}A_0 + \frac{h_\rho^2}{2b_{\rho r}}A_1 + \frac{h_\rho}{2b_{\rho r}}A_2 - \frac{1}{6b_{\rho r}}A_3\right) + \frac{e_i \sin^2\varphi_{\rho r}}{b_{\rho r}} + P_{x\rho r} = \frac{w_{\rho r}}{2b_{\rho r}}\sin 2\varphi_{\rho r}$$

where:

$$\left.\begin{aligned} A_0 &= \sum_{i=\rho}^{n}(P_{xir}-P_{xi\ell}) \\ A_1 &= \sum_{i=\rho}^{n}h_i(P_{xir}-P_{xi\ell}) \\ A_2 &= \sum_{i=1}^{\rho-1}h_i^2(P_{xir}-P_{xi\ell}) \\ A_3 &= \sum_{i=1}^{\rho-1}h_i^3(P_{xir}-P_{xi\ell}) \end{aligned}\right\} \tag{8b}$$

Applying the first of Eq. (8a) from ρ to n and adding the results, then applying the second of Eq. (8a) also from ρ to n and adding the results as well, one obtains two equations which when subtracted from each other give

$$\left(-\frac{a}{6}Q_3+1\right)A_0+\frac{a}{2}Q_2A_1+\frac{a}{2}Q_1A_2-\frac{a}{6}Q_0A_3 = S_0+F_0 \tag{9a}$$

Multiplying the first of Eq. (8a) by h_ρ, computing the results from ρ to n and adding the obtained expressions, then doing the same for the second of Eq (8a), and finally subtracting the two results, one obtains

$$-\frac{a}{6}Q_4A_0+\left(\frac{a}{2}Q_3+1\right)A_1+\frac{a}{2}Q_2A_2-\frac{a}{6}Q_1A_3 = S_1+F_1 \tag{9b}$$

Following the same process, but multiplying at first by h_ρ^2 and then by h_ρ^3, and applying the outcome from 1 to ρ-1, one obtains the following equations

$$\left.\begin{aligned} -\frac{a}{6}R_5A_0+\frac{a}{2}R_4A_1+\left(\frac{a}{2}R_3+1\right)A_2-\frac{a}{6}R_2A_3 &= T_2+D_2 \\ -\frac{a}{6}R_6A_0+\frac{a}{2}R_5A_1+\frac{a}{2}R_4A_2+\left(-\frac{a}{6}R_3+1\right)A_3 &= T_3+D_3 \end{aligned}\right\} \tag{9c-d}$$

where:

$$\left.\begin{aligned} Q_m &= \sum_{i=\rho}^{n}\frac{h_i^m}{b_{ir}}\sin^2\varphi_{ir}+\sum_{i=\rho}^{n}\frac{h_i^m}{b_{i\ell}}\sin^2\varphi_{i\ell} \\ R_m &= \sum_{i=1}^{\rho-1}\frac{h_i^m}{b_{ir}}\sin^2\varphi_{ir}+\sum_{i=1}^{\rho-1}\frac{h_i^m}{b_{i\ell}}\sin^2\varphi_{i\ell} \\ S_m &= \sum_{i=\rho}^{n}\frac{h_i^m}{2b_{ir}}\sin2\varphi_{ir}w_{ir}-\sum_{i=\rho}^{n}\frac{h_i^m}{2b_{i\ell}}\sin2\varphi_{i\ell}w_{i\ell} \\ T_m &= \sum_{i=1}^{\rho-1}\frac{h_i^m}{2b_{ir}}\sin2\varphi_{ir}w_{ir}-\sum_{i=1}^{\rho-1}\frac{h_i^m}{2b_{i\ell}}\sin2\varphi_{i\ell}w_{i\ell} \\ F_m &= e\sum_{i=\rho}^{n}\frac{h_i^m}{b_{ir}}\sin^2\varphi_{ir}+e\sum_{i=\rho}^{n}\frac{h_i^m}{b_{i\ell}}\sin^2\varphi_{i\ell} \\ D_m &= e\sum_{i=1}^{\rho-1}\frac{h_i^m}{b_{ir}}\sin^2\varphi_{ir}+e\sum_{i=1}^{\rho-1}\frac{h_i^m}{b_{i\ell}}\sin^2\varphi_{i\ell} \end{aligned}\right\} \tag{9e}$$

From the system of Eqs. (9a) to (9d), one obtains the terms A_o, A_1, A_2, A_3 and from Eq. (8a) the stresses of the cables, which are

$$\left.\begin{aligned} P_{\rho\ell} &= \frac{\cos\varphi_{\rho\ell}}{b_{\rho\ell}}w_{\rho\ell} - \frac{e\cdot\sin\varphi_{\rho\ell}}{b_{\rho\ell}} - a\left(\frac{h_\rho^3}{6b_{\rho\ell}}A_0 - \frac{h_\rho^2}{2b_{\rho\ell}}A_1 - \frac{h_\rho^2}{2b_{\rho\ell}}A_2 + \frac{h_\rho^3}{6b_{\rho\ell}}A_3\right) \\ P_{\rho r} &= \frac{\cos\varphi_{\rho r}}{b_{\rho r}}w_{\rho r} - \frac{e\cdot\sin\varphi_{\rho r}}{b_{\rho r}} + a\left(\frac{h_\rho^3}{6b_{\rho r}}A_0 - \frac{h_\rho^2}{2b_{\rho r}}A_1 - \frac{h_\rho^2}{2b_{\rho r}}A_2 + \frac{h_\rho^3}{6b_{\rho r}}A_3\right) \end{aligned}\right\} \tag{9f}$$

4.2.2 Dense arrangement of cables

Let us consider next a dense arrangement of cables and that the distances δ_r and δ_ℓ between two adjacent cables satisfy the conditions

$$\delta_\ell \ll \alpha_n - \alpha_1 \quad \text{and} \quad \delta_r \ll \alpha_{2n} - \alpha_{n+1} \tag{10a}$$

In this case, one may consider a distributed load $q_z(x)$ applied from position α_1 to position α_n and from position α_{n+1} to position α_{2n}, which at an arbitrary position x_r is

$$q_{zr}(x_r) = \frac{1}{\delta_r}P_{\rho r}\cos\varphi_{\rho r} \tag{10b}$$

Following the notations of Fig. 8, Eq. (5) become

$$\left.\begin{aligned} \tan\varphi_\ell &= \frac{\ell_\ell - x_\ell}{h_\rho - h_0}, \qquad \tan\varphi_r = \frac{x_r}{h_\rho - h_0} \\ s_\ell &= \frac{\ell_\ell - x_\ell}{\sin\varphi_\ell}, \qquad s_r = \frac{x_r}{\sin\varphi_r} \end{aligned}\right\} \tag{11}$$

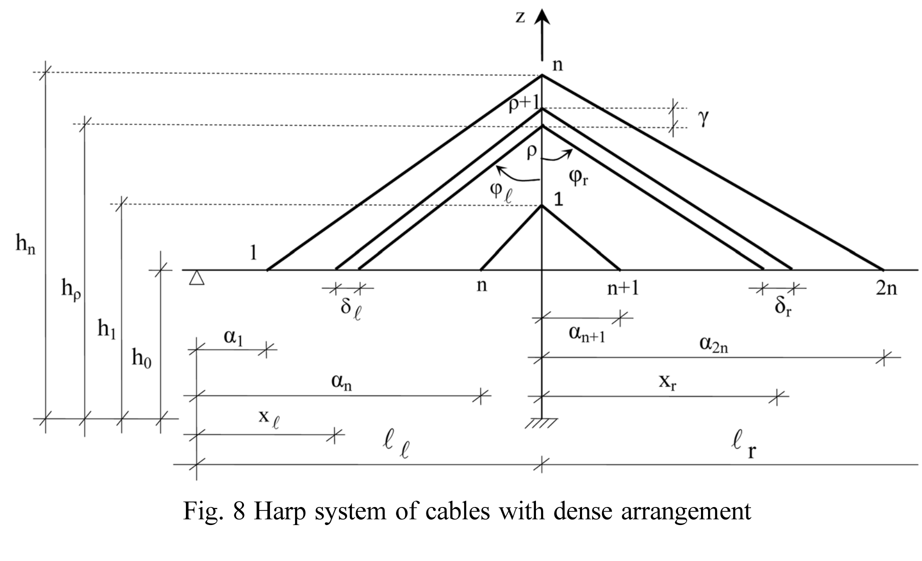

Fig. 8 Harp system of cables with dense arrangement

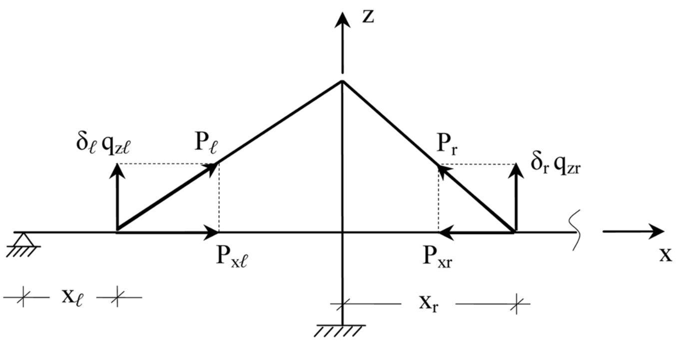

Fig. 9 Pylon stressing due to a dense arrangement of cables

Eq. (7) can be written as follows

$$\left.\begin{array}{l} a = \dfrac{1}{EI_p}, \quad b_\ell = \dfrac{\ell_\ell - x_\ell}{E_c A_c \sin\varphi_\ell}, \quad b_r = \dfrac{x_r}{E_c A_c \sin\varphi_r} \end{array}\right\} \tag{12}$$

One can express x_ℓ and x_r with respect to coordinate z as follows: $\rho = \dfrac{z-h_1}{\gamma}$, $x_\ell = \alpha_n - \rho\delta_\ell$, and $x_r = \alpha_{n+1} + \rho\delta_r$, or finally

$$x_\ell = \alpha_n - \frac{z-h_1}{\gamma}\delta_\ell, \quad x_r = \alpha_{n+1} + \frac{z-h_1}{\gamma}\delta_r \} \tag{13}$$

In addition, from Eq. (10) one has (see Fig. 9)

$$\left.\begin{array}{l} P_{xr} = P_r \sin\varphi_r = \delta_r q_{zr} \tan\varphi_r \\ P_{x\ell} = P_\ell \sin\varphi_\ell = \delta_\ell q_{z\ell} \tan\varphi_\ell \end{array}\right\} \tag{14}$$

Then, Eq. (8b) can be written as follows

$$\left.\begin{array}{l} \bar{A}_0 = \displaystyle\int_z^{h_n} (P_{xr} - P_{x\ell})dx \\ \bar{A}_1 = \displaystyle\int_z^{h_n} z(P_{xr} - P_{x\ell})dx \\ \bar{A}_2 = \displaystyle\int_{h_1}^{z} z^2(P_{xr} - P_{x\ell})dx \\ \bar{A}_3 = \displaystyle\int_{h_1}^{z} z^3(P_{xr} - P_{x\ell})dx \end{array}\right\} \tag{15a}$$

and the system of Eqs. (9a) to (9d) becomes

$$\left.\begin{aligned}\left(-\frac{a}{6}\bar{Q}_3+1\right)\bar{A}_0+\frac{a}{2}\bar{Q}_2\bar{A}_1+\frac{a}{2}\bar{Q}_1\bar{A}_2-\frac{a}{6}\bar{Q}_0\bar{A}_3 &= \bar{S}_0+\bar{F}\\ -\frac{a}{6}\bar{Q}_4\bar{A}_0+\left(\frac{a}{2}\bar{Q}_3+1\right)\bar{A}_1+\frac{a}{2}\bar{Q}_2\bar{A}_2-\frac{a}{6}\bar{Q}_1\bar{A}_3 &= \bar{S}_1+\bar{F}_1\\ -\frac{a}{6}\bar{R}_5\bar{A}_0+\frac{a}{2}\bar{R}_4\bar{A}_1+\left(\frac{a}{2}\bar{R}_3+1\right)\bar{A}_2-\frac{a}{6}\bar{R}_2\bar{A}_3 &= \bar{T}_2+\bar{D}_2\\ -\frac{a}{6}\bar{R}_6\bar{A}_0+\frac{a}{2}\bar{R}_5\bar{A}_1+\frac{a}{2}\bar{R}_4\bar{A}_2+\left(-\frac{a}{6}\bar{R}_3+1\right)\bar{A}_3 &= \bar{T}_3+\bar{D}_3\end{aligned}\right\} \tag{15b}$$

where: $$\left.\begin{aligned}\bar{Q}_m &= \int_z^h\frac{z^m}{b_r}\sin^2\varphi_r dz+\int_z^h\frac{z^m}{b_\ell}\sin^2\varphi_\ell dz\\ \bar{R}_m &= \int_{h_1}^z\frac{z^m}{b_r}\sin^2\varphi_r dz+\int_{h_1}^z\frac{z^m}{b_\ell}\sin^2\varphi_\ell dz\\ \bar{S}_m &= \int_z^h\frac{z^m}{2b_r}\sin 2\varphi_r w_r dz-\int_z^h\frac{z^m}{2b_\ell}\sin 2\varphi_\ell w_\ell dz\\ \bar{T}_m &= \int_{h_1}^z\frac{z^m}{2b_r}\sin 2\varphi_r w_r dz-\int_{h_1}^z\frac{z^m}{2b_\ell}\sin 2\varphi_\ell w_\ell dz\\ \bar{F}_m &= e_i\bar{Q}_m\\ \bar{D}_m &= e_i\bar{R}_m\end{aligned}\right\} \tag{15c}$$

By solving the above system, the coefficients $\bar{A}_0, \bar{A}_1, \bar{A}_2$ and $\bar{A}_3$ are determined and hence, the stresses of the cables can be determined from following relations

$$\left.\begin{aligned}q_{z\ell}(x_\ell) &= \frac{\cos\varphi_\ell}{b_\ell}w_\ell+\frac{e_\ell\sin\varphi_\ell}{b_\ell}-\frac{a\sin\varphi_\ell}{b_\ell}\left(\frac{z^3}{6}\bar{A}_0-\frac{z^2}{2}\bar{A}_1-\frac{z}{2}\bar{A}_2+\frac{1}{6}\bar{A}_3\right)\\ q_{zr}(x_r) &= \frac{\cos\varphi_r}{b_r}w_r+\frac{e_r\sin\varphi_r}{b_r}+\frac{a\sin\varphi_r}{b_r}\left(\frac{z^3}{6}\bar{A}_0-\frac{z^2}{2}\bar{A}_1-\frac{z}{2}\bar{A}_2+\frac{1}{6}\bar{A}_3\right)\end{aligned}\right\} \tag{15d}$$

5. The deformations of the deck

The equation governing the bridge-deck equilibrium is the following

$$E_b I_b w''''(x) = p_{tot}(x) \tag{16}$$

where: E_b is the modulus of elasticity of the bridge-deck, I_b is the moment of inertia of the cross-section of the bridge-deck, $w(x)$ is the total vertical displacement of the deck and

$$p_{tot} = g(x)+p(x)+\sum_\varphi P_\varphi\delta(x-x_\varphi)-q(x,w) \tag{17}$$

In the last Eq. (17), $g(x)$ is the dead load of the bridge, $p(x)$ is the live load, P_φ are concentrated loads (dead or live) at positions $x = x_\varphi$, $q(x, w)$ are the forces due to the cables and $\delta(x)$ is the Dirac-delta function. Therefore, Eq. (16) becomes

$$E_b I_b w''''(x) \;=\; g(x) + p(x) + \sum_{\varphi} P_\varphi \delta(x - x_\varphi) - q(x, w) \tag{18}$$

In order to apply the Galerkin's procedure, one can search for a solution of the form

$$w(x) \;=\; \sum_{i=1}^{n} c_i Z_i(x) \tag{19}$$

Table 1 Case studies - bridge characteristic properties

FAN System				HARP System			
		Bridge I	Bridge II			Bridge I	Bridge II
Slender Pylon $I_p = 100\, I_b$	L_1	150	250	Slender Pylon $I_p = 100\, I_b$	L_1	150	250
	L_2	500	480		L_2	500	480
	L_3	150	250		L_3	150	250
	h_o	130	130		h_o	130	130
	h_1	-	-		h_1	215	215
	h_n	240	240		h_n	240	240
	I_b	1.4	1.4		I_b	1.4	1.4
	δ_l	5.2	8.8		δ_l	5.2	8.8
	δ_r	8.0	9.6		δ_r	8.0	9.6
	γ	-	-		γ	1.0	1.0
	α_1	10	20		α_1	10	20
	α_ρ	140	240		α_n	140	240
	$\alpha_{\rho+1}$	40	60		α_{n+1}	40	60
	$\alpha_{\rho+\kappa}$	240	230		α_{2n}	240	230
		Bridge I	Bridge II			Bridge I	Bridge II
Stiff Pylon $I_p = 1000\, I_b$	L_1	150	250	Stiff Pylon $I_p = 1000\, I_b$	L_1	150	250
	L_2	500	480		L_2	500	480
	L_3	150	250		L_3	150	250
	h_o	130	130		h_o	130	130
	h_1	-	-		h_1	215	215
	h_n	240	240		h_n	240	240
	I_b	1.4	1.4		I_b	1.4	1.4
	δ_l	5.2	8.8		δ_l	5.2	8.8
	δ_r	8.0	9.6		δ_r	8.0	9.6
	γ	-	-		γ	1.0	1.0
	α_1	10	20		α_1	10	20
	α_ρ	140	240		α_n	140	240
	$\alpha_{\rho+1}$	40	60		α_{n+1}	40	60
	$\alpha_{\rho+\kappa}$	240	230		α_{2n}	240	230

where c_i are unknown coefficients to be determined and $Z_i(x)$ are arbitrarily chosen functions of x, which must satisfy the boundary conditions of the deck. In this case, the shape functions of the corresponding continuous beam, which has the same characteristics with the bridge deck but without cables, are chosen. Introducing Eqs. (19) and (17) into Eq. (16), multiplying the outcome successively by Z_1, Z_2, …., Z_n, integrating the results from 0 to L and taking into account the orthogonality conditions of the shape functions, a linear system of n-equations is obtained with unknowns the coefficients c_1, c_2, …,c_n which can be written in the following form

$$G_{i1}c_1 + G_{i2}c_2 + \cdots\cdots + G_{in}c_n = F_i, \quad (i = 1 \text{ to } n) \tag{20}$$

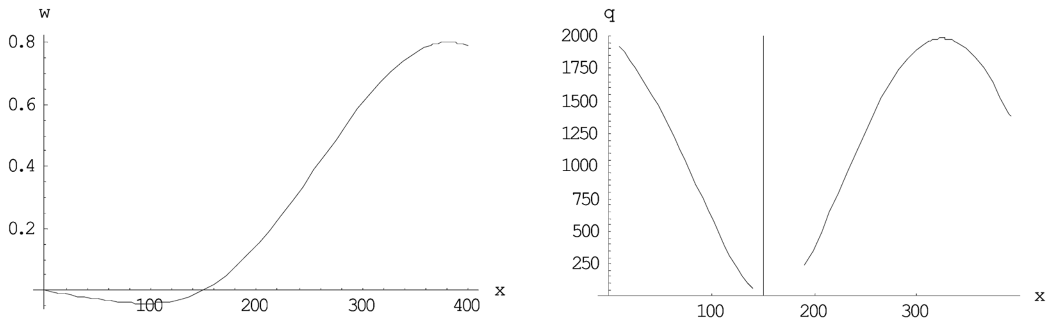

$2e = 0$ m, f=-0.5748 m

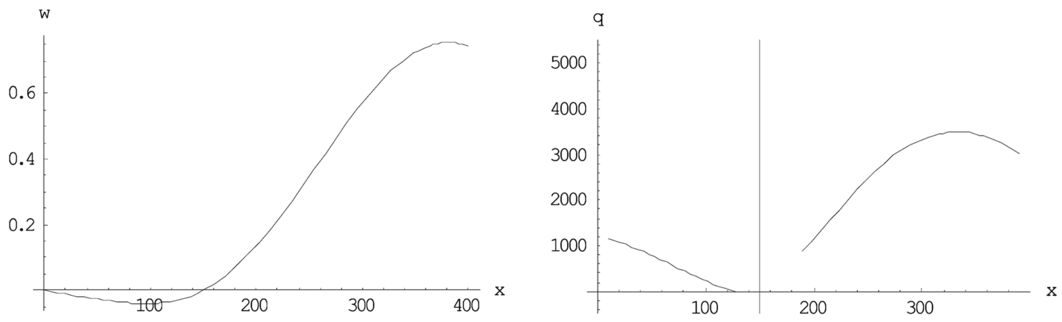

$2e = 0.10$ m, f=0.8938 m

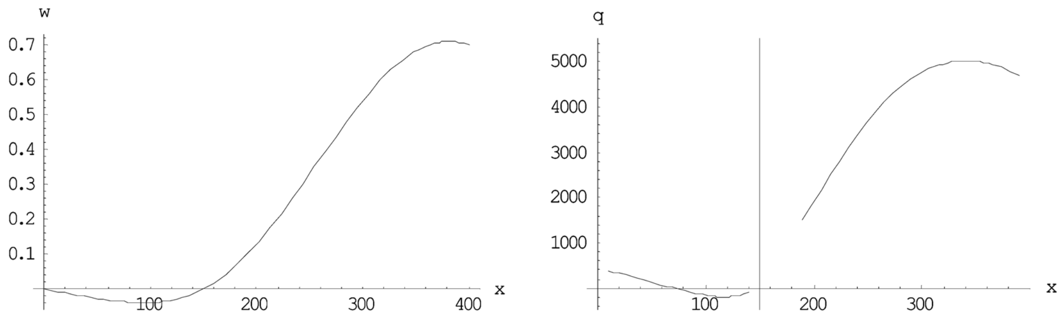

$2e = 0.20$ m, f=2.3627 m

Fig. 10 Deck deformations and cables stresses for type-I bridge with slender pylons
FAN System bridge type-I (spans 150-500-150 m)

Solving the above system, the values of unknowns c_1, c_2, …, c_n are obtained and thus, the expressions for the vertical deformation of the deck as well as the stresses of the cables are derived.

6. Numerical results and discussion

In order to study the influence of the pylons relative displacement on the deck configuration and on the cables stresses, one considers two types of CS-bridge. The first type is built with the fan

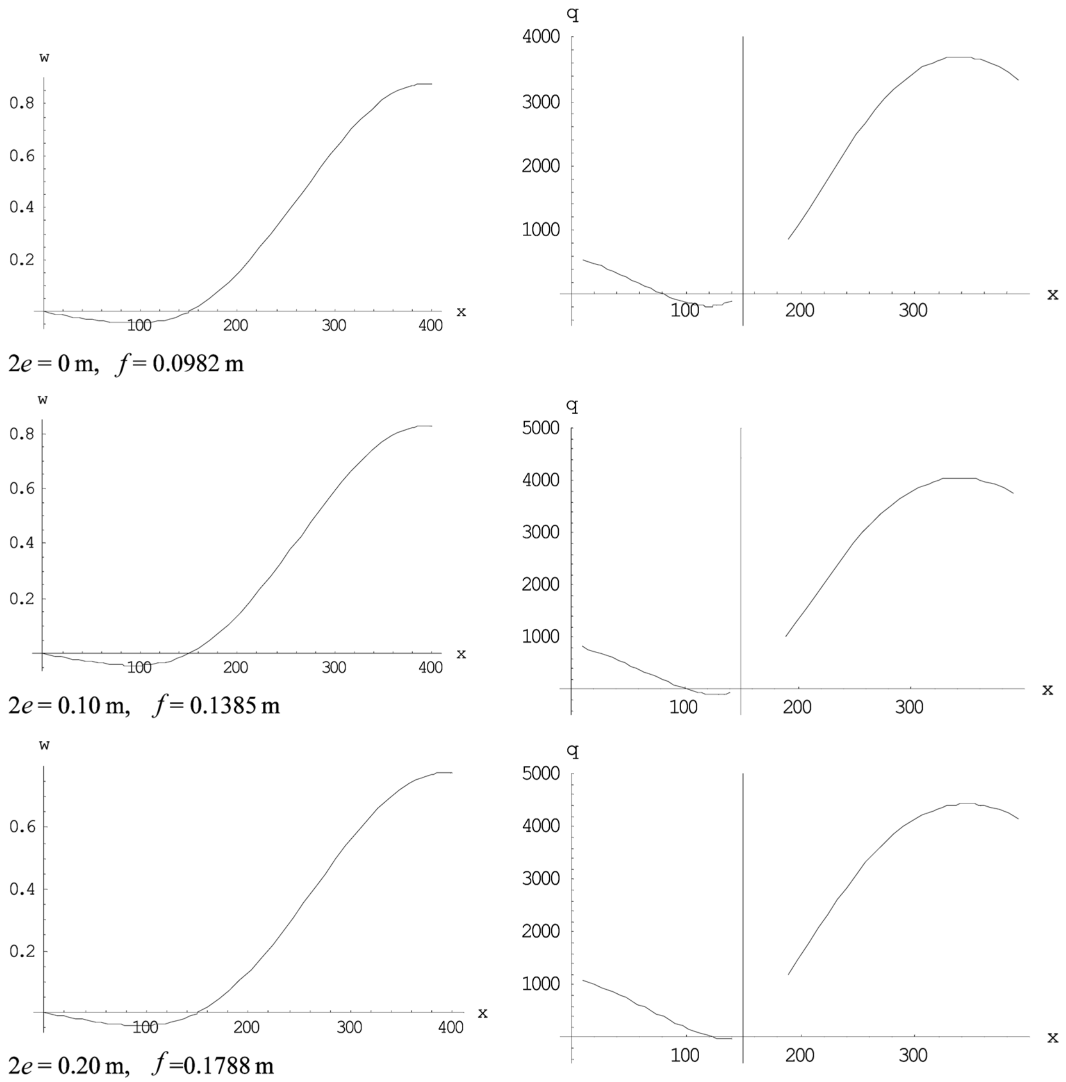

Fig. 11 Deck deformations and cables stresses for type-I bridge with stiff pylons
FAN System bridge type-I (spans 150-500-150 m)

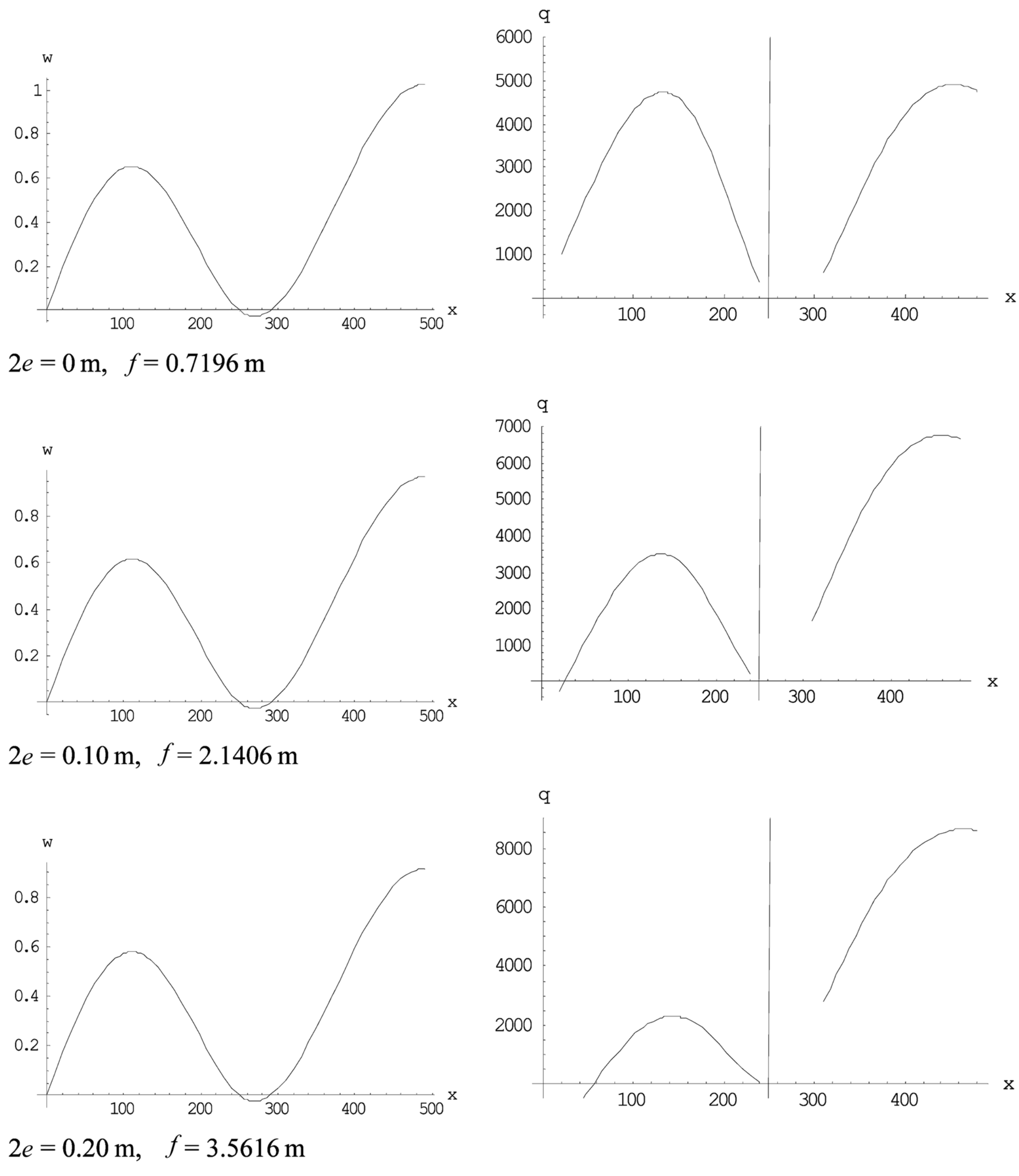

Fig. 12 Deck deformations and cables stresses for type-II bridge with slender pylons
FAN System bridge type-II (spans 250-480-250 m)

system of cables and the second one with the harp system. Each one of them has the characteristics shown in the Table 1. Finally, one also study the deformations of the deck and of the tip of the pylons as well as the cables stresses for displacements of the pylons equal to $2e = e_1 + e_2 = 0$, 0.10 m and 0.20 m.

Fig. 10 shows the deformations and the cables' stresses for a bridge of type I (Table 1) supported

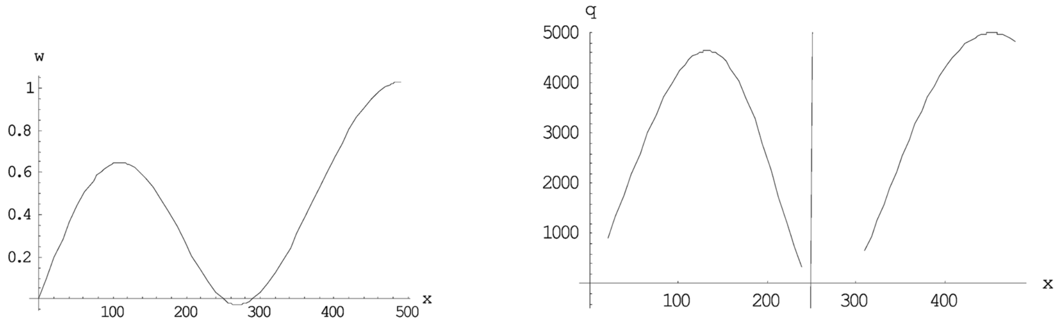

$2e$=0 m, f=0.0783 m

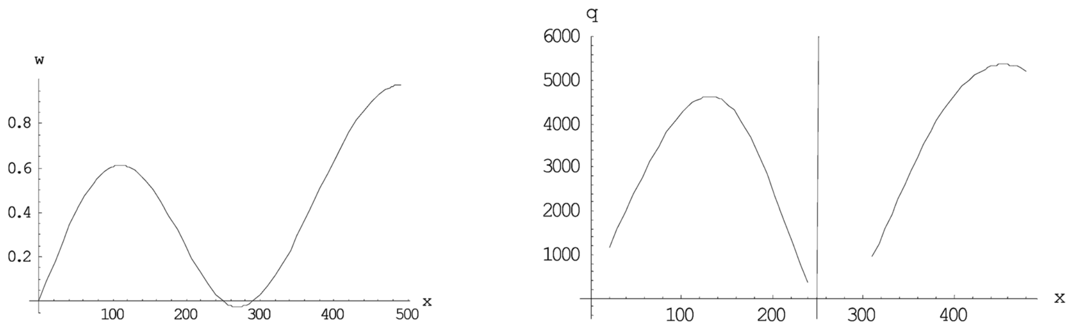

$2e$ = 0.10 m, f=0.1048 m

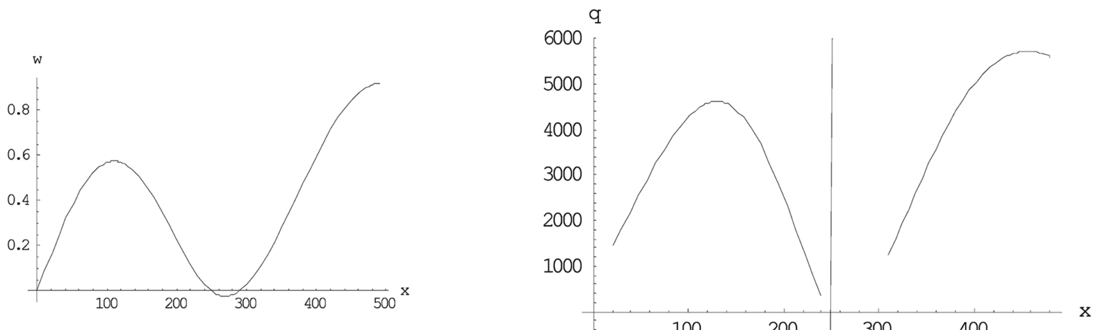

$2e$ = 0.20 m, f=0.1313 m

Fig. 13 Deck deformations and cables stresses for type-II bridge with stiff pylons
FAN System bridge type-II (spans 250-480-250 m)

on slender pylons. As the relative displacement of the pylons increases, the deck's deformations decrease up to ~11% (for $2e = e_1 + e_2 = 20$ cm) while the stresses of the cables of the central span increase up to 150%. At the same time, the cable stresses of the side spans decrease significantly while for $e_1 + e_2 = 20$ cm some of the cables become tensionless. Finally, the tip deformations of the

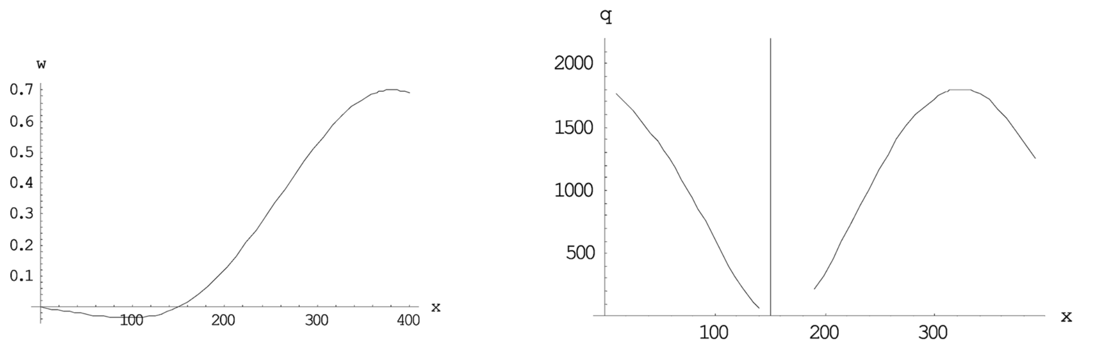

$2e = 0$ m, $f = -0.4129$ m

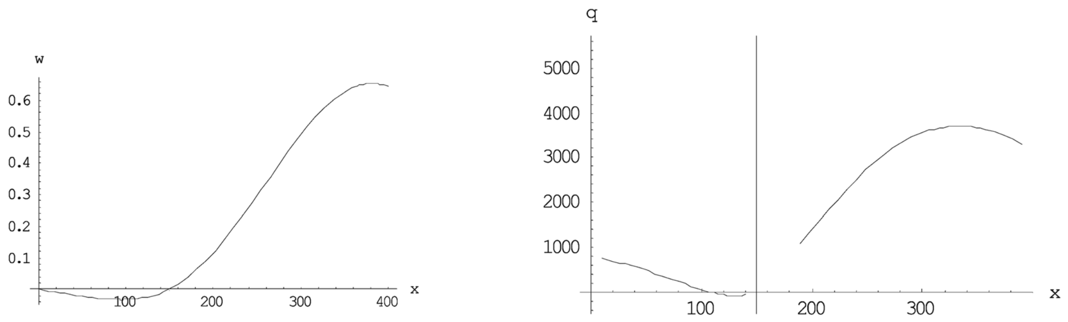

$2e = 0.10$ m, $f = 1.1168$ m

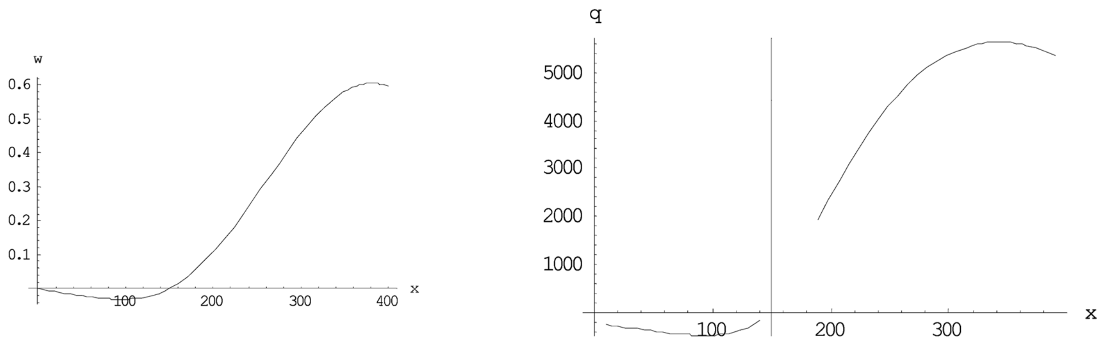

$2e = 0.20$ m, $f = 2.6464$ m

Fig. 14 Deck deformations and cables stresses for type-I bridge with slender pylons HARP System bridge type-I (spans 150-500-150 m)

pylon become unacceptable.

In Fig. 11, one can see the deformations and the stresses of same bridge supported on stiff pylons. The relative displacement of pylons affects less the deck's deformations and mainly the cables stresses. On the other hand, the deformations at the tip of the pylon are acceptable.

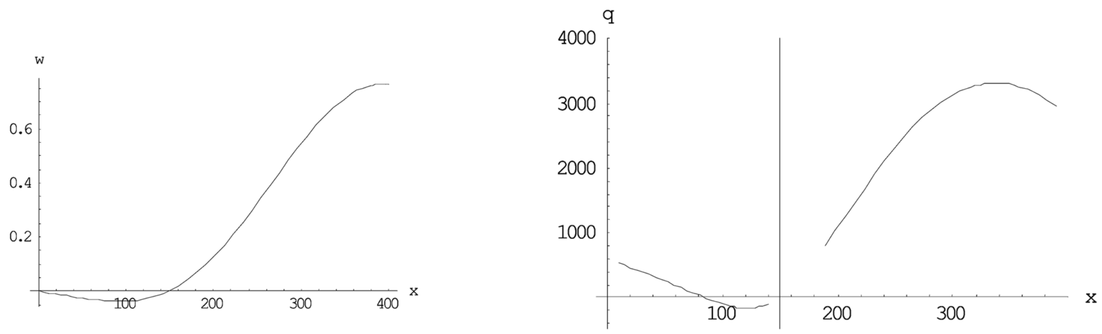

$2e = 0$ m, $f = 0.0751$ m

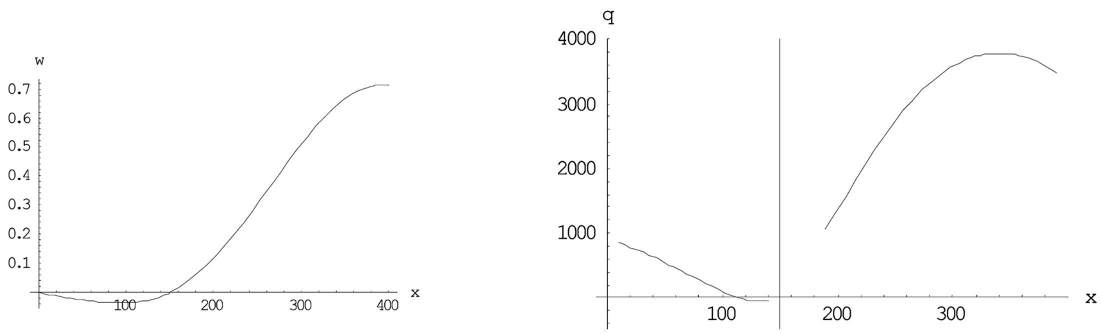

$2e = 0.10$ m, $f = 0.1157$ m

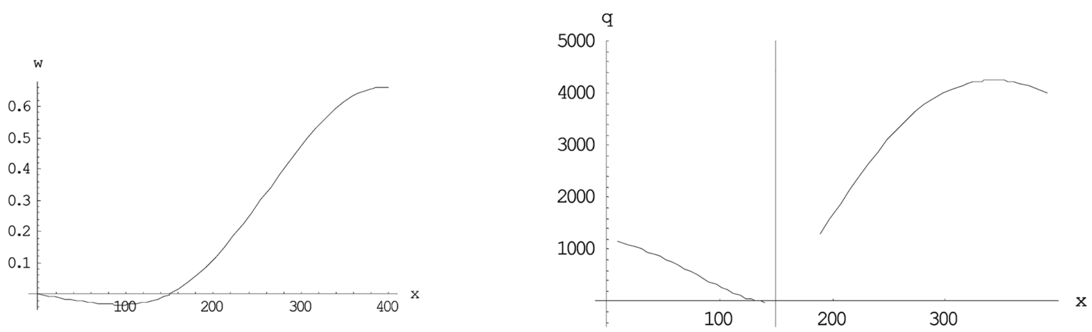

$2e = 0.20$ m, $f = 0.1564$ m

Fig. 15 Deck deformations and cables stresses for type-I bridge with stiff pylons
HARP System bridge type-I (spans 150-500-150 m)

Fig. 12 shows the deformations and the stresses of the cables for a bridge of type II (Table 1) supported on slender pylons. Although the deck's deformations increase as in type I, the cables' stresses increase significantly less than the ones of the previous type. Finally, the pylon's deformations are also unacceptable.

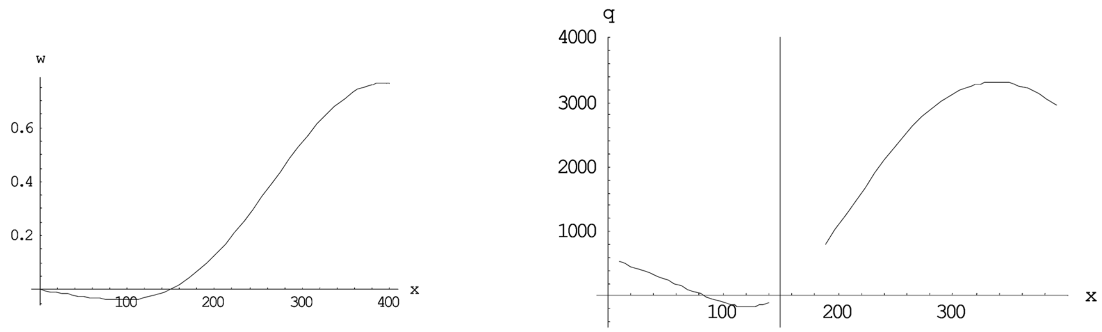

$2e = 0$ m, $f = 0.5528$ m

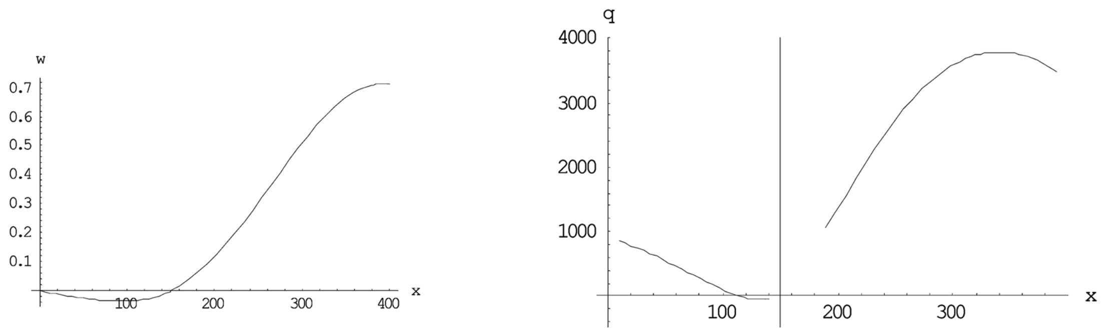

$2e = 0.10$ m, $f = 2.0579$ m

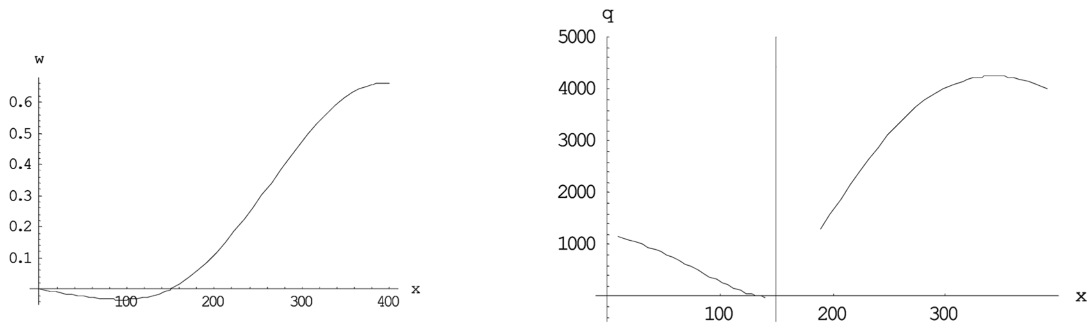

$2e = 0.20$ m, $f = 3.5630$ m

Fig. 16 Deck deformations and cables stresses for type-II bridge with slender pylons
HARP System bridge type-II (spans 250-480-250 m)

In Fig. 13 one can see the results for the same bridge as in Fig. 12 but with stiff pylons. In this case, we also see the favorable influence of the stiff pylons on the deformations and mainly on the cables' stresses.

Finally, the plots of Figs. 14, 15, 16 and 17 show the same results as the above Figs. 10, 11, 12

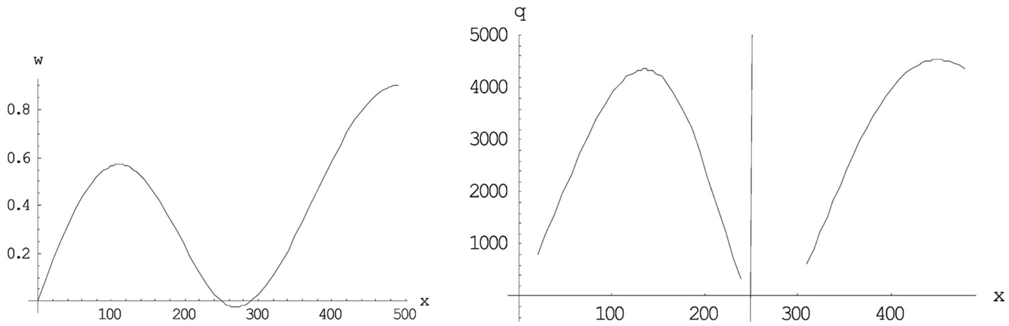

2e = 0 m, f = 0.0577 m

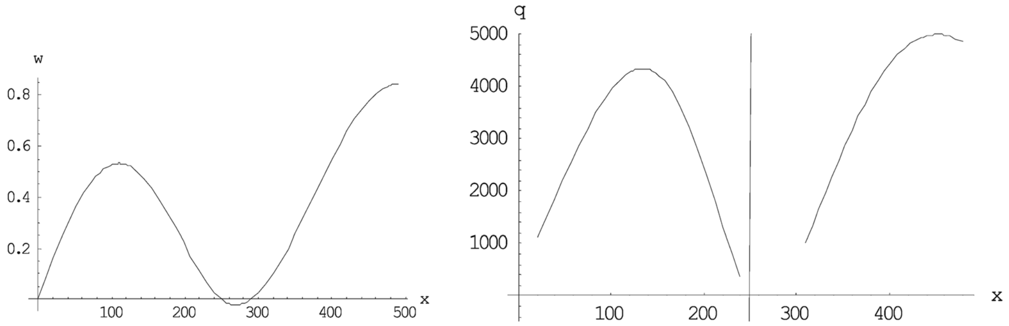

2e = 0.10 m, f =0.0851 m

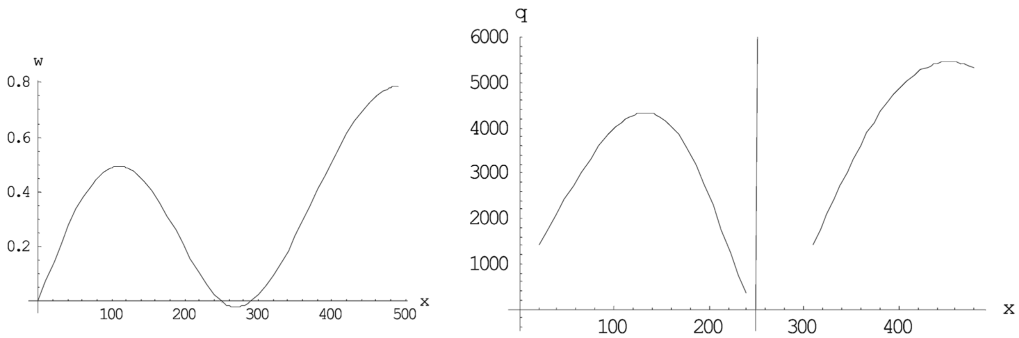

2e = 0.20 m, f =0.1125 m

Fig. 17 Deck deformations and cables stresses for type-II bridge with stiff pylons
HARP System bridge type-II (spans 250-480-250 m)

and 13 but for the bridges of types I and II with a harp system of cables. It is observed that the results are more unfavorable than the ones of the fan system.

7. Conclusions

On the basis of the representative CS-bridge models formulated and analyzed herein, the following conclusions can be drawn:

- Regarding pylons with the same height, the fan system of cables behaves better than the harp one regarding mainly the cables' stresses and the pylons' deformations. The main reason is that the cables' anchor forces are acting higher on the pylon in the fan system than in the harp one, where the cables anchors are distributed over a length $d = \sim h/7$.
- The use of stiff pylons affects significantly the influence of the pylons relative displacement on both systems (fan and harp) and on both types of bridges (I and II).
- Bridges of type II with $L_1 \cong L_2/2$ behave better than bridges of type I, where for high values of pylons' relative displacement $e_1 + e_2$, the cables of the side-spans become inactive.

References

Abdel-Ghaffar, A.M. and Khalifa, M.A. (1991), "Importance of cable vibration in dynamics of cable-stayed bridges", *J. Eng. Mech.*, **117**(11), 2571-2589.

Achkire, Y. and Preumont, A. (1996), "Active tendon control of cable-stayed bridges", *J. Earthq. Eng. Struct. D.*, **25**(6), 585-597.

Bosdogianni, A. and Olivari, D. (1997), "Wind-reduced and rain-induced oscillations of cable-stayed bridges", *J. Wind Eng. Ind. Aerod.*, **64**(2-3), 171-185.

Bruno, D. and Grimaldi, A. (1985), "Non-linear behavior of long-span cable-stayed bridges", *Meccanica*, **20**(4), 303-313.

Bruno, D. and Golotti, V. (1994), "Vibration analysis of cable-stayed bridges", *J. Struct. Ing. Int.*, **4**(1), 23-28.

Chatterjee, P.K., Datta, T.K. and Suruna, C.S. (1994), "Vibration of cable-stayed bridges under moving vehicles", *J. Struct. Ing. Int.*, **4**(2), 116-121.

Ermopoulos, J., Vlahinos, A. and Wang, Y.C. (1992), "Stability analysis of cable-stayed bridges", *Comput. Struct.*, **44**(5), 1083-1089.

Fleming, J.F. (1979), "Non-linear static analysis of cable-stayed bridge structures", *Comput. Struct.*, **10**(4), 986-1000.

Fleming, J.F. and Egeseli, E.A. (1980), "Dynamic behavior of a cable-stayed bridge", *Int. Earthq. Eng. Struct. D.*, **8**(1), 1-16.

Freire, A.M.S., Negrão, J.H.O. and Lopez, A.V. (2006), "Geometrical non-linearities on the static analysis of highly flexible steel cable-stayed bridges", *Comput. Struct.*, **84**(31-32), 2128-2140.

Gimsing, N. (1997), *Cable supported bridges - Concept and design*, 2nd Edition, John Wiley & Sons, Chichester.

Khalil, M.S. (1999), "Non-linear analysis of cable-stayed bridges at ultimate load level", *Can. J. Civil Eng.*, **23**(5), 1111-1117.

Kollbruner, C.F., Hajdin, N. and Stipanic, B. (1980), *Contribution to the analysis of cable-stayed Bridges*, Inst. For Engineering Research Editions, N.48, Schulthess Verlag, Zürich.

Konstantakopoulos, T.G., Michaltsos, G.T. and Sophianopoulos, D.S. (2002), *A simplified model for the study of the lateral-torsional vibration of cable-stayed bridges - Eurodyn 2002*, Springer, Munich.

Leonard, F. (1972), *Bridges*, Architectural Press, London.

Micarelli, L., Moretti, I., Jaubert, M. and Moulouel, H. (2006), "Fracture analysis in the south-western Corinth rift (Greece) and implications on fault hydraulic behavior", *Tectonophysics*, **426**(1-2), 285-296.

Michaltsos, G.T. (2001), "A simplified model for the dynamic analysis of cable-stayed bridges", *Facta Universitatis*, **3**(11), 185-204.

Michaltsos, G.T., Ermopoulos, J.C. and Konstantakopoulos, T.G. (2003), "Preliminary design of cable-stayed bridges for vertical static loads", *J. Struct. Eng. Mech.*, **16**(1), 1-15.

Michaltsos, G.T. (2005), *Stability of a cable-stayed bridge's pylon, under time-depended loading*, Collection of papers in memory of Academician P.S. Theocharis. Inst. of Mechanics Problems and Academy of Sciences, Russia, Inst. Of Mechanics of Nat. Acad. of Sciences, Armenia.

Michaltsos, G.T., Raftoyiannis, I.G. and Konstantakopoulos, T.G. (2008), "Dynamic stability of cable-stayed bridge pylons", *Int. J. Struct. Stabil. Dyn.*, **8**(4), 627-643.

Mozos, C.M. and Aparicio, A.C. (2010), "Parametric study on the dynamic response of cable-stayed bridges to the sudden failure of a stay. Part I: Bending moment acting on the deck", *Eng. Struct.*, **32**(10), 3288-3300.

Nazmy, A.S. and Abdel-Ghaffar, A.M. (1990), "Non-linear earthquake response analysis of long-span cable-stayed bridges", *Earthq. Eng. Struct. D.*, **19**(1), 45-62.

Tapponnier, P., Ryerson, F.J., Van der Woert, J., Meriaux, A.S. and Lasserre, C. (2001), "Long-term slip rates and characteristic slip: keys to active fault behaviour and earthquake hazard", *Earth Planet. Sci.*, **333**(9), 483-494.

Troitsky, M.C. (1988), *Cable-stayed bridges - Theory and design*, 2^{nd} edition, B.S.P. Professional Books, London.

Virgoreux, M. (1999), "Recent evolution of cable-stayed bridges", *J. Eng. Struct.*, **21**(8), 737-755.

Wang, P.H., Liu, M.Y., Huang, Y.T. and Lin, L.C. (2010), "Influence of lateral motion of cable-stayed bridges", *Struct. Eng. Mech.*, **34**(6), 719-738.

Xanthakos, P.P. (1994), *Theory and design of bridges*, John Wiley & Sons, New York.